

许涵, 程仲景, 刘演, 等. 海洋沉积记录的南海北部地区末次冰期野火历史及其驱动机制[J]. *Quaternary Sciences*, 2025, 45(2):546-558.  
XU Han, CHENG Zhongjing, LIU Yan, et al. Marine sedimentary records reveal paleofire history and its driving mechanisms in the northern South China Sea during the Last Glacial[J]. *Quaternary Sciences*, 45(2):546-558.

DOI: 10.11928/j.issn.1001-7410.2025.02.18

CSTR: 32086.14.j.issn.1001-7410.2025.02.18

# 海洋沉积记录的南海北部地区末次冰期野火历史及其驱动机制\*

许涵<sup>1</sup>, 程仲景<sup>2</sup>, 刘演<sup>1</sup>, 翁成郁<sup>2</sup>,

Stephan STEINKE<sup>3</sup>, Mahyar MOHTADI<sup>4</sup>, 孙千里<sup>1</sup>

(1. 华东师范大学河口海岸国家重点实验室, 上海 200241; 2. 同济大学海洋地质全国重点实验室, 上海 200092; 3. 厦门大学海洋生物地球化学全国重点实验室, 厦门 361005; 4. 不来梅大学 MARUM 海洋环境研究中心, 不来梅 D28395, 德国)

**摘要:** 火在地球系统中起着至关重要的作用, 对气候变化、植被演替和碳循环有重大影响, 但其影响因素复杂多样, 在全球范围内有很强的空间异质性。在热带/亚热带亚洲地区, 野火的驱动机制仍然存在较多不同的认识。本研究通过对南海北部 GeoB16602 站点的末次冰期 85 个海洋沉积物样品(钻孔深度范围是 9.47~2.91 m)进行炭屑分析, 并结合孢粉分析结果重建该区域过去 65~18 ka 的古火灾演化序列, 揭示古火灾与古气候和古植被的联系。结果表明, GeoB16602 站点的炭屑记录在过去 65~18 ka 变化显著。在整体趋势上, 随着气候变干, 草本植物持续扩张, 火灾呈现增长态势。在此背景下, 虽然氧同位素 3 期岁差的波动幅度很小, 但野火仍然清晰地表现出与之吻合的约两万年周期性变化, 且野火事件的峰值往往对应岁差低值期, 即夏季太阳辐射最强且冬季最弱的时期。这可能表明与生态系统(如草本/木本比例的变化)相比, 火灾对于太阳辐射驱动的气候季节性变化更为敏感。

**关键词:** 植被; 炭屑; 古火灾; 季节性; 岁差

**中图分类号:** Q914.9, P722.7

**文献标识码:** A

**文章编号:** 1001-7410(2025)02-546-13

## 0 引言

野火作为生物圈中的重要自然现象, 与气候、植被模式和人类活动密切相关, 对植被演替和陆地碳循环的维持起着重要作用<sup>[1-3]</sup>。20 世纪野火产生的温室气体、尘埃等导致全球陆地表面平均温度上升了 0.18 °C<sup>[4]</sup>。近年来加拿大、澳大利亚和希腊等国都发生了多次大规模森林火灾, 造成了巨大的生态破坏和经济损失。野火发生时向大气中排放大量有害污染物和温室气体, 对全球气候和人类健康造成不利影响<sup>[5]</sup>。随着全球气温不断上升, 未来火灾风险隐患可能持续增长<sup>[6-8]</sup>, 对陆地生态系统的安全和社会的可持续发展构成严重威胁。因此, 野火已经成为全球变化研究的关键议题。但不同区

域野火发生频率、强度、周期等存在较大差异, 而各区域的野火机制也存在较多不同的认知, 例如: 在非洲西北部的 3 个海洋钻孔的炭屑记录显示, 不同纬度(9°N、15°N、21°N)过去 50 ka 野火变化规律并不一致, 可能与水文气候差异有关<sup>[9]</sup>。因此, 重建长时间尺度上的古火历史, 对于理解区域内野火的响应机制、保障当地社会稳定与经济发展具有重要意义。

南海北部地区位于东亚季风区, 是珠江入海泥沙的主要沉积区<sup>[10-11]</sup>。晚第四纪以来沉积速率相对较高, 沉积地层保存完好, 因此是重建长时间尺度高分辨率古环境变化的理想区域。目前该地区已经开展了诸多第四纪植被、气候变化的重建研究<sup>[12-19]</sup>, 但较少关注气候变化下的野火发生过程和

2024-12-25 收稿, 2025-01-20 收修改稿

\* 国家重点研发计划项目(批准号:2023YFF0803902)、国家自然科学基金面上项目(批准号:42376061 和 42371013)和上海市科委科技项目(批准号:TQ20220101)共同资助

第一作者简介: 许涵, 女, 23 岁, 硕士研究生, 自然地理学专业, E-mail: hanxu0368@163.com

通讯作者: 程仲景, E-mail: magnolia\_czj@tongji.edu.cn; 刘演, E-mail: liuyan@sklec.ecnu.edu.cn

机制。且关于野火的研究常见于全新世时期,而全新世期间剧烈的人类活动可以直接改变火灾发生的强度和频率,所以很难直接在沉积记录中准确识别火灾发生的自然驱动机制<sup>[20-23]</sup>。在末次冰期(MIS 2~4),人类活动影响相对微弱,并且全球水文气候发生了多次千年尺度的大幅波动<sup>[24-25]</sup>,因而成为理解气候变化下的植被与野火演化及其相互关系的理想时间窗口。

炭屑是植物组织不完全燃烧或高温分解产生的一种深褐色或黑色无机碳化合物,燃烧温度通常在 280~500 °C<sup>[26-27]</sup>。由于野火受气候和植被的控制,因此炭屑记录也间接反映出水文气候和植被变化<sup>[28]</sup>。目前已有大量研究利用炭屑进行古火演化研究,但其复杂的驱动机制导致对植被-气候-野火响应的认识仍存在较大分歧<sup>[29-33]</sup>,同时也导致气候模型预测存在很大的不确定性<sup>[34]</sup>。

因此,本研究拟通过对南海北部 GeoB16602 钻孔末次冰期(65~18 ka)沉积物中的炭屑浓度进行分析,并结合已发表的孢粉组合记录<sup>[35-36]</sup>,重建该区域末次冰期的野火历史,探讨南海北部野火演化规律及其驱动机制,进而为预测和应对极端气候条件下中国热带/亚热带地区野火发生风险和生态系统管理提供理论参考。

## 1 研究区概况

南海是热带西太平洋最大的半封闭边缘海,北邻中国大陆,南属西太平洋暖池,西部集水盆地靠近青藏高原,东部通过巴士海峡与西太平洋相连,对气候变化极为敏感(图 1a)。南海北部主要受控于东亚季风气候,冬季(11月至2月)盛行东北季风,夏季(5月至8月)盛行西南季风。季风区夏季湿热,冬季温和,年平均气温约为 20~27 °C。降水季节差异大,夏季降水量通常是冬季的 4~10 倍。在 GeoB16602 站点(图 1a),河流沉积物主要来自华南地区,特别是珠江流域和台湾南部,少量来自吕宋岛<sup>[37-39]</sup>。在末次冰期,海平面最多下降到-130 m 左右,南海北部露出了约 39×10<sup>4</sup> km<sup>2</sup> 的陆地,海岸线向海延伸了约 200 km<sup>[40]</sup>。珠江水系延伸流经裸露的大陆架,使得这一时期的 GeoB16602 站点接收了更多来自中国南方的沉积物<sup>[35,37]</sup>。目前,南海北部周围的植被被划分为 3 个区系:中亚热带常绿阔叶林、南亚热带常绿阔叶林以及热带季雨林和热带雨林<sup>[35,41]</sup>。现代观测发现,亚热带湿润区的火灾多发生在冬季,尤其是 2 月份,而夏季发生的火灾相对较少<sup>[42]</sup>。

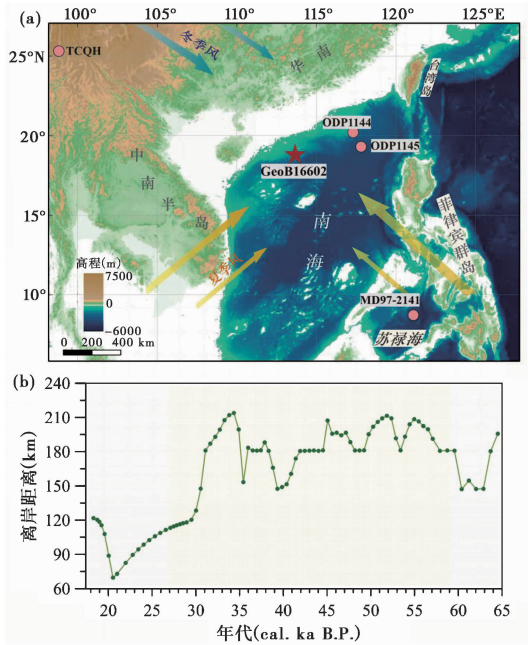


图 1 GeoB16602 站点位置及研究区位置图

(a) 相对海平面为 -130 m 的 MIS 2 期间古地形(在现代地形上叠加海平面数据得出,现代地形数据来自 www.gebco.net),白色区域表示这一海平面下露出的大陆架;(b) 根据 LR04 海平面曲线计算的不同时期的 GeoB16602 站点与海岸线距离<sup>[37]</sup>

Fig. 1 Location of the study area and GeoB16602 site. (a) Paleotopography during MIS 2 with a relative sea level of -130 meters (data from www.gebco.net), where white areas represent the exposed continental shelf; (b) Distances from GeoB16602 to the coastline at different periods calculated based on the LR04 sea level curve<sup>[37]</sup>

## 2 材料与方法

### 2.1 样品年代序列与采集

GeoB16002 站点(18°57'N, 113°42'36"E; 水深 953 m)位于中国南海西北部,于 2012 年 RV SONNE SO-221" INVERS" 航次<sup>[43]</sup>期间共采集 1 个重力岩芯和 3 个 MeBo 岩芯。在已发表的文献资料中,前人使用 AnalySeries 2.0.8 程序<sup>[44]</sup>将底栖有孔虫  $\delta^{18}\text{O}$  数据与全球叠加曲线 LR04<sup>[37]</sup>进行了比对建立了初步的年龄框架<sup>[35]</sup>;并结合岩芯上部 5.62 m 的 15 个 AMS <sup>14</sup>C 测年(0~36.8 ka)进行了更精细的校正<sup>[37]</sup>。在此年代框架下,本研究的炭屑分析采集了 85 个样本,深度范围是 9.47~2.91 m,年龄跨度为 65~18 ka,采样间距为 5~10 cm,平均年代分辨率约为 600 年,所有样本均采用标准的氢氟酸法进行处理<sup>[36,45]</sup>。

### 2.2 炭屑统计及浓度计算

已有研究通常通过以下 3 个炭屑参数重建古火

历史。首先是描述火灾强度或频率的炭屑数量(浓度或通量)<sup>[26-27]</sup>,浓度越高则火灾强度越大频率越高。其次是炭屑粒径,许多研究发现粗粒炭屑( $CC_{large}$ )在火烧地点数公里内沉积<sup>[46-48]</sup>,可代表地方性火活动事件;而细粒炭屑( $CC_{small}$ )传播距离相对更远则主要反映区域性火活动事件<sup>[49-52]</sup>,因此可通过  $CC_{large}/CC_{small}$  的比率定性地描述这种随距离变化的粒度分级<sup>[53-55]</sup>。最后是炭屑形态,即通过计算炭屑颗粒的长宽比,将近圆形炭屑表示木本燃料,长形炭屑表示草本燃料<sup>[28,56-58]</sup>。

本研究在 400 倍光学显微镜下完成对炭屑的测量与统计计数,每个样品至少测量 500 粒,通过外加石松孢子计算样品中不同粒级及形态的炭屑浓度。本研究根据炭屑长轴长度将其分为 3 个等级: 10 ~ 50  $\mu\text{m}$  (细粒)、50 ~ 100  $\mu\text{m}$  (中粒)、> 100  $\mu\text{m}$  (粗粒),计算  $CC_{large}$  (> 50  $\mu\text{m}$ ) 和  $CC_{small}$  (10 ~ 50  $\mu\text{m}$ ) 的比率来分析沉积点与炭屑源区的相对距离变化<sup>[50,59]</sup>。此外,本研究参考已发表文献将炭屑颗粒的长短轴比值分为 2 类:> 2.5 的长形炭屑(long)和 < 2.5 的圆形炭屑(round),分别指代草本和木本燃烧的炭屑<sup>[60-61]</sup>,并计算  $CC_{long}/CC_{round}$  比率来分析野火燃料(草类/木本)的百分比<sup>[28,55,62]</sup>。

### 2.3 炭屑浓度数据分析

在古环境研究中,时间序列的预测分析往往受到样品分布不均匀性的影响<sup>[63]</sup>。广义加法模型(Generalized Additive Models, 简称 GAM)能够估计非线性趋势并提供变化幅度的准确估计,成为古环境时间序列趋势估计的一种良好的替代方法<sup>[63]</sup>。对于每个粒级的炭屑浓度及总浓度,在 R3.6.3 软件中使用 R 包 mgcv 的 GAM 函数<sup>[63]</sup>进行趋势拟合以识别出具有相似变化趋势的时期。

近些年来,全球古火研究的快速发展与炭屑分析新方法及统计模型的出现密不可分。借助炭屑传播-沉积机理的炭屑统计模型(CharAnalysis),可以快速提取炭屑记录的野火信息(火事件 fire events; 火间隔期 fire return intervals, 简称 FRI; 火频率 fire frequency)<sup>[64]</sup>。其原理为:将炭屑记录( $C_{int}$ )分解为低频( $C_{back}$ )和高频( $C_{peak}$ )成分,再使用局部定义的 95%、99% 或 99.9% 噪声得到炭屑记录的阈值( $C_{threshold}$ )用以分离火信号( $C_{fire}$ )和噪声( $C_{noise}$ ),最终得到火事件并计算火灾频率和火间隔期,实现峰值检测以重建“地方性”火灾历史的目的。本研究选择 95% 的置信区间进行阈值分析,将  $C_{peak}$  定义为

$C_{int}$  与  $C_{back}$  之差。在 Matlab 中运行 CharAnalysis 程序<sup>[64]</sup>包对炭屑总浓度进行野火历史重现,分析火事件和火频率发生的情况。

为探讨本站位已发表的花粉类群<sup>[35-36]</sup>与炭屑浓度之间的关系,在 Origin 2021 中进行了主成分分析(PCA),根据氧同位素阶段对数据进行分组。使用 PAST 软件<sup>[65]</sup>提供的用于不均匀采样数据的 Lomb 周期图算法<sup>[66]</sup>,对炭屑总浓度进行了频谱分析检查火事件是否存在周期性的变化。此外,还对炭屑总浓度进行连续小波变换<sup>[67]</sup>进一步验证野火事件的周期性。

## 3 研究结果

GeoB16602 站点沉积物中的平均炭屑总浓度为 63414.64 粒/ $\text{cm}^3$ ,其中细粒炭屑平均浓度为 46934.6 粒/ $\text{cm}^3$ (图 2),中粒炭屑平均浓度为 13693.5 粒/ $\text{cm}^3$ ,粗粒炭屑平均浓度 2786.4 粒/ $\text{cm}^3$ 。尽管细粒、中粒以及粗粒炭屑浓度值存在

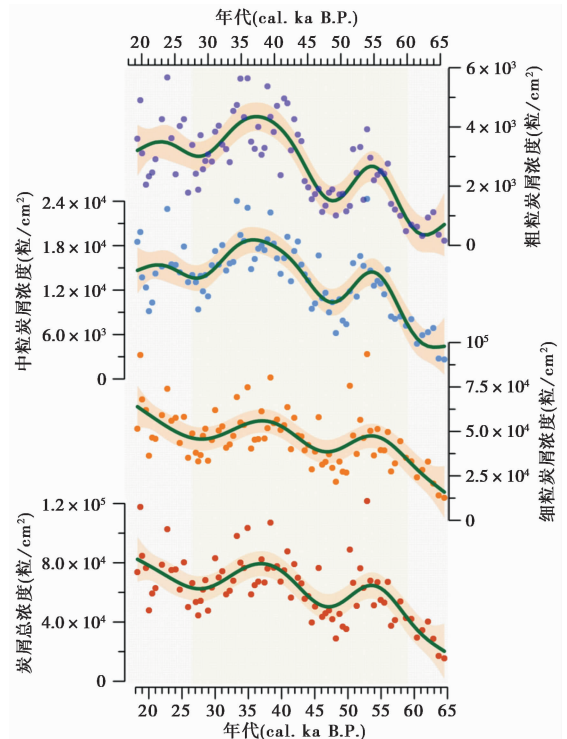


图 2 GeoB16602 站点炭屑浓度

彩色点表示每个样品的浓度,连续曲线表示基于 GAM 的趋势线,红色阴影包络线表示趋势的 95% 置信区间

Fig. 2 Charcoal concentration at GeoB16602 site. Colored points represent the concentration of each sample, while the continuous lines indicate trend lines based on Generalized Additive Models (GAM). The red shaded envelope represents the 95% confidence interval for the trends

较大差异,但它们之间的变化趋势非常相似(图 2)。细粒炭屑浓度与炭屑总浓度的变化趋势最为接近,这是由于细粒炭屑因粒度较小易于传播,所以来源最广,颗粒数量占总数最多(约占62.2%~91.8%)。整体而言,炭屑浓度从 65 cal. ka B.P. 到末次冰盛期(LGM)呈现增多的趋势。而在此背景之下,GAM 趋势线显示炭屑总浓度具有明显的周期性变化,在 55.0 ~ 53.5 cal. ka B.P.、39 ~ 37 cal. ka B.P. 以及 18 cal. ka B.P. 分别出现最大值,表示此时生物量燃烧显著增加,野火发生频繁。炭屑总浓度的 Lomb 谱分析(置信度 99%),连续小波变换也肯定了约 19 ka 的周期性变化(图 3)。炭屑通量与浓度表现出相对一致的变化规律,表明沉积速率对上述观察的影响不大。

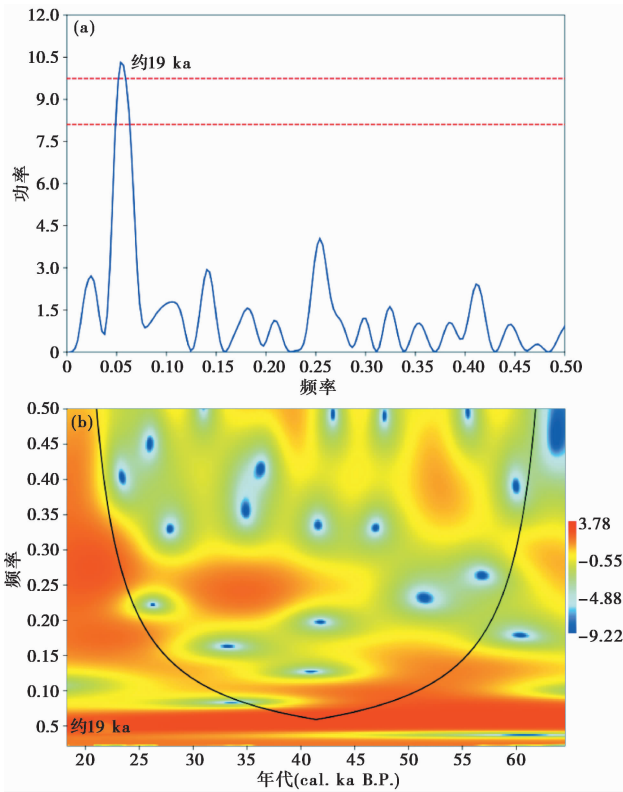


图 3 炭屑总浓度 Lomb 谱分析和小波分析图

(a) 非均匀采样数据的 Lomb 周期分析反映约 19 ka 周期信号<sup>[65]</sup>,其中,红线表示  $P < 0.01$  和  $P < 0.05$  的显著性水平; (b) 小波变换反映约 19 ka 周期信号在整个分析时间段内都显著存在<sup>[67]</sup>

Fig. 3 Lomb spectral analysis and wavelet analysis of total charcoal concentration. (a) Lomb periodogram algorithm for nonuniformly sampled data reveals a ca. 19 ka periodic signal<sup>[65]</sup>. The red lines indicate  $P$  values of 0.01 and 0.05; (b) Wavelet transform reveals that the ca. 19 ka periodic signal is significantly present throughout the entire period<sup>[67]</sup>

对炭屑浓度(图 4a)进行 CharAnalysis 分析得到模型插值后的炭屑通量(图 4b),并据此识别出

14 起火事件( $N_{\text{FRI}} = 13$ )(图 4b),火频率在 0~3 次/5 ka 之间波动(图 4d),平均 FRI 为 3620 年,野火强度波动大(图 4c)。MIS 4 晚期, FRI 很短,但峰值量级低即野火强度弱。进入 MIS 3 之后,火事件的峰值量级增大。特别是在大约 53 ka,发生了一起高强度野火。在 39~31 ka 期间, FRI 较短,峰值量级相对低,即此时发生高频率低强度的野火。LGM 时期识别的 2 起野火事件强度高, FRI 约为 2000 年。

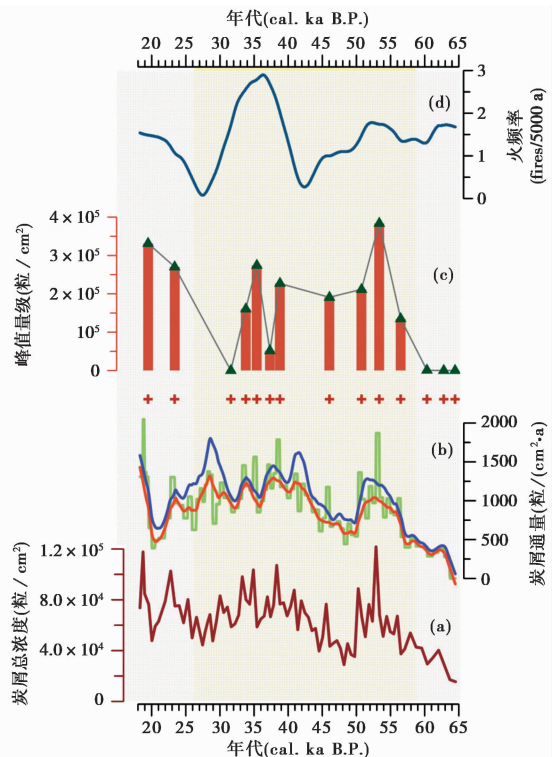


图 4 炭屑总浓度 CharAnalysis 分析结果

(a) 炭屑总浓度; (b) CharAnalysis 重建的炭屑通量(绿色代表  $C_{\text{int}}$ ; 紫色代表  $C_{\text{threshold}}$ ; 橙色代表  $C_{\text{back}}$ ; 红色十字代表识别的“野火事件”); (c) 野火事件的炭屑峰值量级(粒/cm<sup>2</sup>, 表示火事件强度); (d) CharAnalysis 重建的火频率(fires/5000 a)

Fig. 4 Results of CharAnalysis on total charcoal concentration. (a) Total charcoal concentration; (b) Charcoal flux reconstructed by CharAnalysis (green represents  $C_{\text{int}}$ ; purple represents  $C_{\text{threshold}}$ ; orange represents  $C_{\text{back}}$ ; red crosses indicate identified “fire events”); (c) Magnitude of charcoal peaks associated with wildfire events (pieces/cm<sup>2</sup>, indicating fire event intensity); (d) Fire frequency(fires/5000 a);

在 PCA 分析中(图 5),前两个轴解释了花粉数据<sup>[35-36]</sup>总方差的 36.9%,其中 24.9%由 PC1 解释,12.0%由 PC2 解释。在第一主轴上负极成分多为温暖湿润的植物类型,比如热带山地雨林属种罗汉松属

(*Podocarpus*)、陆均松属(*Dacrydium*)，以及喜暖喜湿的蕨类植物如桫欏属(*Cyathea*)和芒萁属(*Dicranopteris*)；与之相对的，正极成分则多为生长在更寒冷干燥气候中的植物类型，如一些温带的落叶木本水青冈属(*Fagus*)、鹅耳枥属(*Carpinus*)、枫杨属(*Pterocarya*)，生长习性更为广域的栎属(*Quercus*)，以及象征干旱的草地植物禾本科(*Poaceae*)，而炭屑浓度与第一主轴正极成分变化一致。

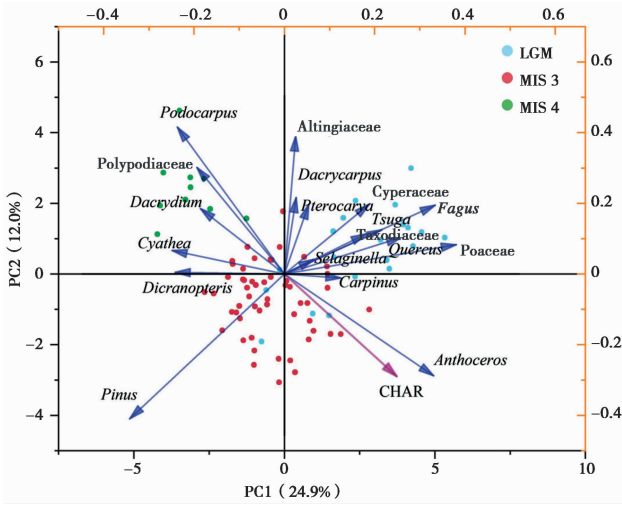


图5 炭屑浓度和花粉分类群的主成分分析(PCA)

黑色坐标轴代表样本得分图坐标，橙色坐标轴代表花粉分类群及炭屑载荷图坐标

Fig. 5 Principal Component Analysis (PCA) of charcoal concentration and pollen taxa. The black axes represent the sample score plot coordinates, the orange axes represent the pollen taxa and charcoal loading plot coordinates

## 4 讨论

火的时空变化受复杂的气候变化(温度、降水)、燃料(类型、数量)和点火源(闪电、火山活动和人类活动)的影响<sup>[6, 68-69]</sup>。气候条件既可直接影响点火条件而改变野火驱动机制,也可间接通过改变植被生产力、可燃性等条件影响火灾发生<sup>[28]</sup>。本研究讨论过去 65~18 ka 长时间尺度的炭屑数据,为了解野火机制及其与气候和植被的相互关系提供重要信息。

### 4.1 GeoB16602 站位炭屑来源

炭屑颗粒形成后,主要通过大气和水流运输,最终沉积在土壤、湖泊或海洋环境中<sup>[70-71]</sup>。已有研究表明,同一岩芯的炭屑和花粉来源相似<sup>[34]</sup>。先前研究发现 GeoB16602 站位岩芯顶部样本的花粉组成与珠江流域的现代植被相符<sup>[35]</sup>,来自台湾和海

南岛山区的花粉贡献极少。多个南海北部孢粉传播机制的研究也发现此区域的孢粉主要来自珠江和南海东北部<sup>[72-73]</sup>。因此,珠江流域是 GeoB16602 站位炭屑颗粒的主要来源。大气颗粒扩散模拟研究发现,>1000  $\mu\text{m}$  的颗粒就近沉积,而>500  $\mu\text{m}$  的颗粒通过空气传播的距离也相对较近,>125  $\mu\text{m}$  的颗粒多数落在 7 km 范围内,通过空气传播能超过这一范围的大颗粒物沉积较少<sup>[50]</sup>。根据重建的站位离岸距离变化历史所示<sup>[37]</sup>,即使在海平面最低时期 GeoB16602 站点与海岸线的距离也高达数十千米(图 1b),这表明沉积物中的粗粒炭屑主要是由水流运输。考虑到孢粉的颗粒大小与中、细粒级的炭屑颗粒相当(10~100  $\mu\text{m}$ ),可作为中、细粒级炭屑颗粒传播方式的参考。现代层沉积物的分析结果表明,珠江是南海北部花粉沉积最主要的来源<sup>[74-75]</sup>。其他海区的相关研究同样显示,当周边存在大型河流时,风力搬运的贡献可忽略不计<sup>[76-78]</sup>。因此推测中、细颗粒炭屑同样以河流注入为主。大、中、小这 3 个粒级炭屑的一致变化也在很大程度上肯定了这一推论。

### 4.2 南海北部野火演变规律及驱动机制分析

#### 4.2.1 野火长期趋势

海洋陆源沉积物浓度通常受海平面波动的影响,海平面下降时,站点离岸更近,搬运距离减少,导致陆源物质浓度升高<sup>[37]</sup>。GeoB16602 站位炭屑浓度 65~18 ka 整体增加的趋势(图 6g)可能与海平面从氧同位素 3 期到末次冰盛期的整体下降趋势有关<sup>[79]</sup>(图 6d),即随着海平面降低,站点与岸线距离缩短<sup>[37]</sup>(图 1b)更有利于炭屑的搬运,导致炭屑总浓度升高。但海平面并不能全部解释炭屑浓度的变化,尤其是在氧同位素 4 期(65~60 ka),虽然海平面相对较低,但炭屑浓度也处于较低水平。从整体趋势来看,反映草本与木本相对比例的  $CC_{\text{long}}/CC_{\text{round}}$ <sup>[60, 80-81]</sup> 在 65~18 ka 期间呈现逐渐增大(草本燃料增多)的趋势(图 6e),这与同钻孔的草本植物花粉含量持续增多的趋势相吻合<sup>[36]</sup>(图 6f)。可见,炭屑与花粉两个独立指标均指向(古)珠江流域内草本植物从 65 ka 到 18 ka 持续扩张的态势。在华南地区,草本植物的多少(代表了森林的开阔度)往往与气候整体的干燥程度相关<sup>[82]</sup>,换言之 GeoB16602 的植被记录显示源区气候从 65 cal. ka B.P. 到 18 cal. ka B.P. 呈持续变干趋势。虽然尚不能解释这一记录与附近其它降雨记录的差异,例如云南腾冲青海湖的降雨重建结果显示

氧同位素 4 期气候显著变干, 氧同位素 3 期变得非常湿润, 之后降水才缓慢减少<sup>[83]</sup> (图 6b), 推测这一差异可能与海洋沉积复杂的来源有关。但考虑到炭屑与孢粉的来源基本一致, 从同一钻孔的炭屑和植被记录的高度相关性可以推断, 南海北部的野火随着气候变冷变干、草地扩张<sup>[36, 84-85]</sup> (图 6a、6c 和 6f), 呈现更为活跃的态势, TCQH 的炭屑记录也同样反映火活动受控于干冷气候变化<sup>[86]</sup>。而这一点也体现在 PCA 分析结果中, 炭屑明显与一众喜干冷的植物花粉高度相关 (图 5)。更长时间尺度上跨冰期旋回的其它野火记录也支持这一结论, 如南海北部 ODP1144 孔炭屑记录<sup>[87]</sup>、亚北极太平洋黑碳记录<sup>[88]</sup> 以及黄土古土壤序列中的黑碳记录<sup>[32]</sup> 均显示冰期炭屑浓度升高, 间冰期降低。

现代野火卫星数据显示, 野火在密闭的森林体

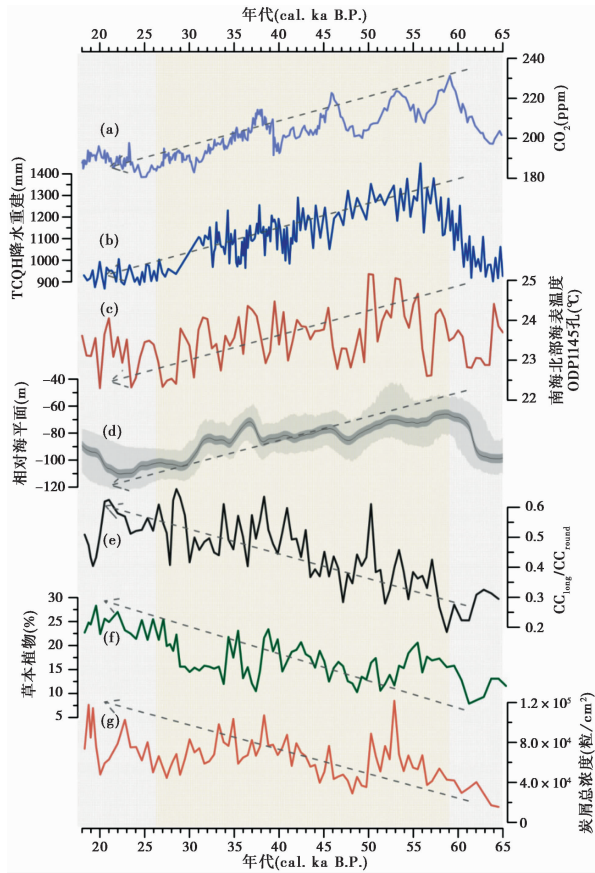


图 6 野火事件长期驱动机制对比

(a)  $\text{CO}_2$ <sup>[84]</sup>; (b) TCQH 降水重建<sup>[83]</sup>; (c) 南海北部海面温度 (ODP1145 孔)<sup>[85]</sup>; (d) 相对海平面高度<sup>[79]</sup>; (e)  $\text{CC}_{\text{long}}/\text{CC}_{\text{round}}$ <sup>[60, 80-81]</sup>; (f) 草本植物含量<sup>[36]</sup>; (g) 炭屑总浓度

Fig. 6 Comparison of long-term driving mechanisms of wildfire. (a)  $\text{CO}_2$ <sup>[84]</sup>; (b) Precipitation reconstruction from TCQH<sup>[83]</sup>; (c) Sea surface temperature in the northern South China Sea (ODP1145 core)<sup>[85]</sup>; (d) Relative sea level<sup>[79]</sup>; (e)  $\text{CC}_{\text{long}}/\text{CC}_{\text{round}}$ <sup>[60, 80-81]</sup>; (f) Herbaceous plant<sup>[36]</sup>; (g) Total charcoal concentration

系中较少出现, 而在相对开阔的森林中, 草本植物更容易被引燃, 野火发生的频率更大<sup>[89-90]</sup>。地表可燃物是森林火灾发生、蔓延的重要条件和物质基础, 由地表可燃物引起的地表火是森林发生火灾的重要原因。地表可燃物主要包括枯枝落叶层、草本和灌木<sup>[91]</sup>。可燃物垂直结构上的连续性是地表火转为树冠火的主要原因, 地表火通过梯状可燃物蔓延至树冠, 发展为高强度的树冠火<sup>[92-93]</sup>。在南海北部地区, 干旱的气候一方面可以增加生态体系中地表可燃物的比例, 另一方面干燥气候本身可能也更容易导致火灾发生。

#### 4.2.2 野火的岁差周期

除上述长时间尺度的整体变化外, 炭屑指示的生物质燃烧每间隔约 19 ka 出现一段峰值 (图 7h)。

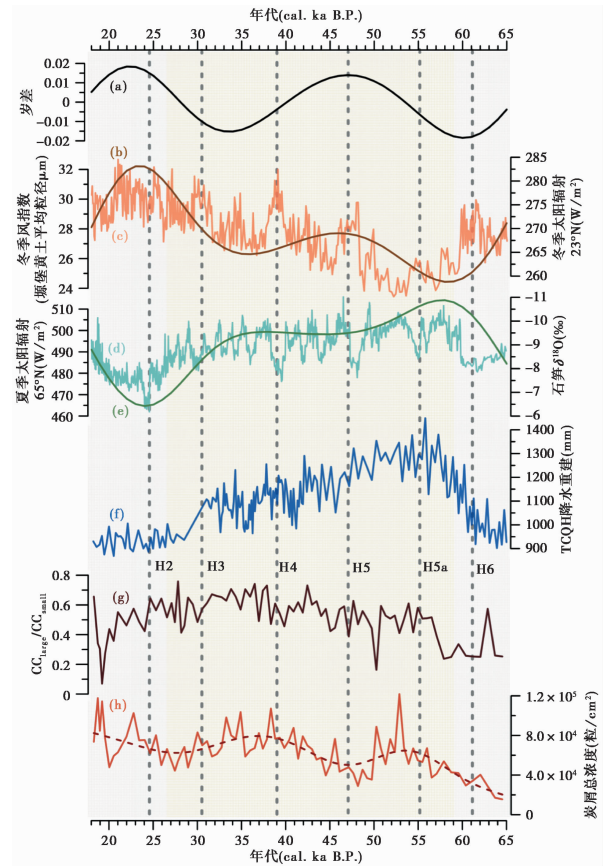


图 7 野火事件千年尺度驱动机制对比

(a) 岁差<sup>[94]</sup>; (b)  $23^\circ\text{N}$  冬季太阳辐射 (12 月 21 日)<sup>[94]</sup>; (c) 冬季风指数 (塬堡黄土平均粒径)<sup>[95]</sup>; (d)  $\delta^{18}\text{O}$  从石笋<sup>[96]</sup>; (e)  $65^\circ\text{N}$  夏季太阳辐射 (6 月 21 日)<sup>[94]</sup>; (f) TCQH 降水重建<sup>[83]</sup>; (g)  $\text{CC}_{\text{large}}/\text{CC}_{\text{round}}$ ; (h) 炭屑总浓度

Fig. 7 Comparison of driving mechanisms of wildfire on a millennial scale. (a) Precession<sup>[94]</sup>; (b) Winter solar insolation at  $23^\circ\text{N}$  (December 21)<sup>[94]</sup>; (c) Winter monsoon index (average grain size of Yuanbao loess)<sup>[95]</sup>; (d)  $\delta^{18}\text{O}$  from stalagmites<sup>[96]</sup>; (e) Summer solar insolation at  $65^\circ\text{N}$  (June 21)<sup>[94]</sup>; (f) Precipitation reconstruction from TCQH<sup>[83]</sup>; (g)  $\text{CC}_{\text{large}}/\text{CC}_{\text{round}}$ ; (h) Total charcoal concentration

这一周期性变化总体与海平面变化相反,即在相对高海平面时期炭屑浓度反而更高,例如 50~55 ka 期间,这些变化更多反映的是火灾活动而非沉积搬运过程的变化。19 ka 周期通常被认为是岁差旋回的体现,广泛存在于南海的其他气候代用指标中,例如有孔虫氧碳同位素<sup>[97]</sup>、蛋白石<sup>[98]</sup>以及一些地球化学指标<sup>[99]</sup>。一些其它地区的夏季风指标,例如石笋氧同位素<sup>[100]</sup>和黄土磁化率<sup>[32,101-103]</sup>,也都揭示了清晰的岁差周期变化。然而,本文的研究时段是整个末次冰期旋回中岁差变化幅度最小的时期。无论是石笋<sup>[96]</sup>(图 7d)还是其它季风记录,如腾冲青海的年均降雨重建结果<sup>[83]</sup>(图 7f),在这个时期都很难清晰辨识出周期性的岁差变化,本钻孔中草本植物含量的变化亦是如此<sup>[36]</sup>(图 6e和 6f)。

但 GeoB16602 野火记录中 35~40 ka 以及 50~55 ka 两段炭屑高值期较为清晰地对应于北半球夏季太阳辐射的高值期(冬季太阳辐射的低值期)<sup>[94]</sup>(图 7e和 7b)。而在低纬度地区,太阳日射的季节变化受岁差的显著影响,并且在南、北半球的影响相反<sup>[104]</sup>。一种可能的解释为,在岁差周期中,野火直接响应于太阳辐射引起的降雨季节性变化,而非年均降雨量的变化。许多研究表明,以草本植物为燃料的野火在很大程度上取决于降雨季节性,因为降水的季节分配影响着草本植物的生长及可燃性<sup>[104-108]</sup>。在南海北部地区,在岁差低值期时(图 7a),夏季太阳辐射增强<sup>[94]</sup>(图 7e),ITCZ 北移,降雨增多,有利于生物质燃料的生长和累积;而对应的北半球冬季太阳辐射更弱,东亚冬季风增强<sup>[95]</sup>(图 7c),气候变得更为干燥,更利于可燃生物物质的点燃,二者叠加导致火灾更易发生(图 7h)。相反地,在岁差最大值时北半球季节性减弱<sup>[94]</sup>(图 7a),相对凉爽的夏季限制植被生长而温和的冬季降低了可燃物的干燥程度和点火条件<sup>[109]</sup>,因此野火活动较弱,例如在 47 ka B.P. 和 28 ka B.P. 炭屑浓度均出现最低值。图 6 和 7 中的古气候记录来看,在这种微弱的岁差周期中,太阳辐射驱动的小幅季节性气候变化可能并不足以引起年均降雨以及生态系统的显著转变,如草地向森林的转变;但足以通过对生态系统的细微影响,如草本植物在生长季积累的生物质,引起野火强度的改变。换言之,野火可能是一个对气候季节性更为敏感的环境因子。

#### 4.2.3 野火对千年气候事件的响应

在千年尺度上,GeoB16602 的野火记录与气候

突变信号的对应关系相对复杂。在末次冰期存在一系列显著的全球性气候快速振荡事件,比如北大西洋冰筏碎屑引起的 Heinrich 事件<sup>[24,110]</sup>,期间大量淡水注入促使北大西洋经向翻转流减弱或中断,使全球热量交换发生变化。H 事件在我国的古气候记录中有十分清楚地显示<sup>[111-112]</sup>,例如黄土粒度记录<sup>[95]</sup>显示 H 事件期间冬季风显著增强(图 7c),而石笋记录<sup>[96]</sup>显示 ITCZ 南移,夏季风减弱(图 7d)。在我们的记录中,Heinrich 变冷事件 H3、H4、H5 时期,炭屑浓度似乎略有升高,反映炭屑源区距离的  $CC_{large}/CC_{round}$  比值(图 7g)总体处于高值期。而其它 Heinrich 事件 H2、H5 a、H6 时期,炭屑总体浓度并无明显变化。这种并不清晰的对应关系,一方面可能与我们样品较低的时间分辨率以及较粗略的年龄模式有关;另一方面也可能反映了在不同的气候背景下,如上文所论证的长期趋势,再叠加岁差旋回时,野火事件对 H 事件复杂的响应过程。总之,H 事件与野火之间的响应机制还需要更多更高分辨率的沉积记录研究。

#### 4.2.4 野火活动与植被类型

此外,不同木本植物的可燃性不同,对火灾的发生发展也会产生一定影响<sup>[113-114]</sup>。对 GeoB16602 站位过去 65~18 ka 的炭屑总浓度、孢粉相对丰度和  $CC_{long}/CC_{round}$  比率之间的关系进行 Pearson 相关性分析发现,炭屑浓度与山地雨林针叶树负相关( $r=-0.44$ ),但与草本植物( $r=0.32$ )、热带/亚热带常绿树( $r=0.24$ )正相关,与温带落叶林( $r=0.0069$ )关联性极低(图 8)。火灾频率和强度与雨林的负相关性以及与草本植物的正相关性正如上文所言,可能与植被密闭度有关。雨林林冠茂密郁闭性好,地表可燃物水分蒸发减弱可燃物质含水率高且林间空气湿度大,抑制地表火的发生<sup>[93,115]</sup>;而草本植物通过增加地表可燃生物量增大火灾发生机率。但炭屑总浓度与热带/亚热带常绿树更为相关而与温带落叶林关系不大难以理解。落叶树种落叶时间多发生在秋季,常绿树则是在春季新叶萌发时,老叶同时从林冠脱落。而春季逐渐回暖蒸发量增加,掉落的枯叶含水量低更易燃<sup>[116]</sup>,这可能是在该地区常绿林相对落叶林更容易引发火灾的一种解释。

#### 4.2.5 野火记录可能指示的人类活动

除了不同时间尺度上的气候变化,人类活动也是一个影响火灾发生的潜在因素<sup>[117-118]</sup>。尽管前文已经指出,本文之所以关注冰期这个时段就是为了

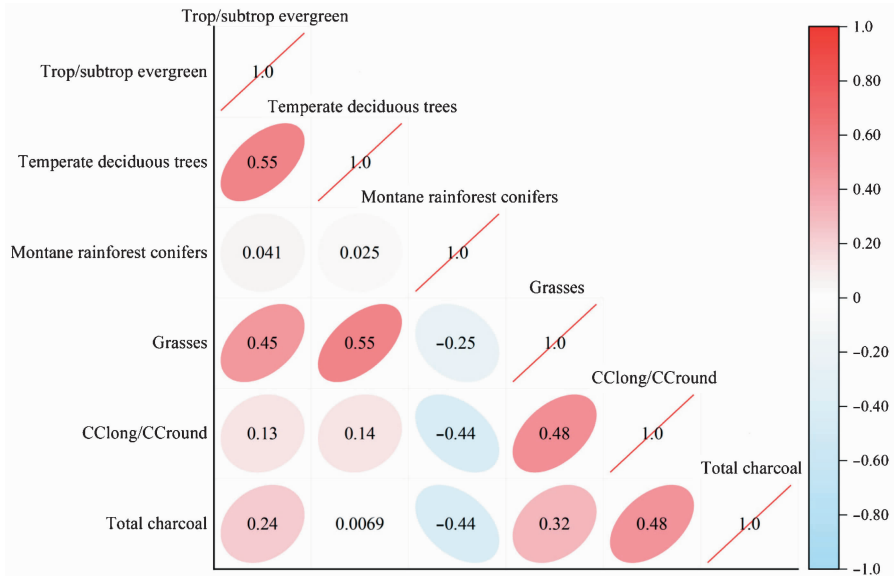


图 8 炭屑、植被与  $CC_{long}/CC_{round}$  的相关性分析

Fig. 8 Correlation analysis of charcoal, vegetation, and  $CC_{long}/CC_{round}$ .

避免人类活动的强烈扰动,但出露的陆架可能是早期古人类迁移的重要路线,并且这些人类活动的影响不能完全忽略。Beaufort<sup>[119]</sup>在对苏禄海 MD97-2141 钻孔野火研究中发现,51 cal. ka B.P. 左右有一个炭屑浓度的峰值;Thevenon 等<sup>[120]</sup>应用多种方法分析了位于赤道的海洋沉积物重建西赤道太平洋过去 36 万年的野火历史,同样发现 53~43 cal. ka B.P. 左右炭屑大量增加;Kershaw 等<sup>[121]</sup>指出,这些边缘海记录中的炭屑峰值与早期现代人抵达东南亚的时间一致,是人类活动的体现。出露的南海陆架同样是旧石器时代现代人经华南向高纬地区(朝鲜半岛、日本岛)迁移的重要路径<sup>[122]</sup>。GeoB16602 的炭屑记录中,CharAnalysis 分析结果识别出一起强度较大的野火事件出现在 53 cal. ka B.P. 左右(图 4c),炭屑浓度在 53 cal. ka B.P. 左右也有一个相对异常的高值(图 4a),且这个事件并不在岁差极小值时期,与千年尺度气候事件也没有显著的关联。从时间上看,这些事件也与东南亚的记录有一定程度的一致性。因此,我们推测 53 cal. ka B.P. 的野火信号可能与低海平面时期陆架上古人类活动有关。但其真实性以及背后机制,仍需要更多高分辨率、以及更多迁移路线上的其它记录来确认。无论如何,海洋沉积物在这方面可能具有很大的研究潜力。

## 5 结论

本文研究 GeoB16602 站位的炭屑数据,通过炭

屑的粒径、浓度提取沉积物中区域性火灾和地方性火灾的信号,通过炭屑的形态分析火灾燃料信息,重建了末次冰期(65~18 ka)的古火演化历史。在整体趋势上,炭屑浓度随着气候变干,草本植物扩张,呈现增多趋势。与此同时,炭屑浓度存在清晰的约 19 ka 周期变化,其高值期对应于岁差低值期。这一变化在同时期的植被、降雨以及季风记录中并不显著。我们推断相较于植被或年均降雨量,火灾可直接响应于岁差引起的气候季节性变化。具体而言,岁差低值期,北半球热带/亚热带地区夏季太阳辐射更强(冬季太阳辐射更弱),即气候季节性增强时,火灾更易发生。此外,在本记录中,千年尺度气候事件、植物属种组成、古人类活动与野火的关系较为模糊,尚需其它高分辨率的记录,以及更大空间尺度上的对比研究加以确认。本记录体现了在不同时间尺度、不同气候变幅中,野火与气候之间不同的响应模式,需要在未来野火的预测工作中加以考虑。

## 参考文献 (References):

- [1] Vander Werf G R, Randerson J T, Collatz G J, et al. Continental-scale partitioning of fire emissions during the 1997 to 2001 El Niño/La Niña Period[J]. Science, 2004, 303(5654):73-76.
- [2] Bowman D M J S, Balch J K, Artaxo P, et al. Fire in the Earth system[J]. Science, 2009, 324(5926):481-484.
- [3] Abatzoglou J T, Williams A P, Boschetti L, et al. Global patterns of interannual climate-fire relationships [J]. Global Change Biology, 2018, 24(11):5164-5175.
- [4] Li F, Lawrence D M, Bond-Lamberty B. Impact of fire on global land

- surface air temperature and energy budget for the 20th century due to changes within ecosystems[J]. *Environmental Research Letters*, 2017, 12(4). doi: 10.1088/1748-9326/aa6685.
- [5] 董千里, 孟鑫, 宫继成, 等. 大气中黑碳的暴露及人体健康效应研究进展[J]. *科学通报*, 2024, 69(6):703-716.  
Dong Qianli, Meng Xin, Gong Jicheng, et al. A review of advances in black carbon exposure assessment and health effects[J]. *Chinese Science Bulletin*, 2024, 69(6):703-716.
- [6] 刘恋. 新生代增温情景下自然火历史的研究[J]. *第四纪研究*, 2019, 39(5):1289-1296.  
Liu Lian. The natural fire history during warming periods of Cenozoic[J]. *Quaternary Sciences*, 2019, 39(5):1289-1296.
- [7] Westerling L A. Increasing western US forest wildfire activity: Sensitivity to changes in the timing of spring[J]. *Philosophical transactions of the Royal Society of London. Series B: Biological Sciences*, 2016, 371(1696). doi: 10.1098/rstb.2015.0178.
- [8] Gaboriau D M, Remy C C, Girardin M P, et al. Temperature and fuel availability control fire size/severity in the boreal forest of central Northwest Territories, Canada[J]. *Quaternary Science Reviews*, 2020, 250. doi: 10.1016/j.quascirev.2020.106697.
- [9] Moore H R, Crocker A J, Belcher C M, et al. Hydroclimate variability was the main control on fire activity in Northern Africa over the last 50,000 years[J]. *Quaternary Science Reviews*, 2022, 288. doi: 10.1016/j.quascirev.2022.107578.
- [10] 蔡观强, 彭学超, 张玉兰. 南海沉积物物质来源研究的意义及其进展[J]. *海洋科学进展*, 2011, 29(1):113-121.  
Cai Guanqiang, Peng Xuechao, Zhang Yulan, et al. The significances of and advances in the study of sediment sources in the South China Sea[J]. *Advances in Marine Science*, 2011, 29(1):113-121.
- [11] 邵磊, 赵梦, 乔培军, 等. 南海北部沉积物特征及其对珠江演变的响应[J]. *第四纪研究*, 2013, 33(4):760-770.  
Shao Lei, Zhao Meng, Qiao Peijun, et al. The characteristics of the sediment in northern South China Sea and its response to the evolution of the Pearl River[J]. *Quaternary Sciences*, 2013, 33(4):760-770.
- [12] Sun X J, Li X. A pollen record of the last 37 ka in deep sea core 17940 from the northern slope of the South China Sea[J]. *Marine Geology*, 1999, 156(1-4):227-244.
- [13] Sun X J, Li X, Luo Y L, et al. The vegetation and climate at the last glaciation on the emerged continental shelf of the South China Sea[J]. *Palaeogeography, Palaeoclimatology, Palaeoecology*, 2000, 160(3):301-316.
- [14] Sun X J, Luo Y L, Huang F, et al. Deep-sea pollen from the South China Sea: Pleistocene indicators of East Asian monsoon[J]. *Marine Geology*, 2003, 201(1-3):97-118.
- [15] Sun X J, Luo Y L. Pollen record of the last 280 ka from deep sea sediments of the northern South China Sea[J]. *Science in China (Series D: Earth Sciences)*, 2001, 44(10):879-888.
- [16] Luo Y L, Sun X J. Vegetation evolution and millennial-scale climatic fluctuations since Last Glacial Maximum in pollen record from northern South China Sea[J]. *Chinese Science Bulletin*, 2005, 50(8):793-799.
- [17] Wang X M, Sun X J, Wang P X, et al. Vegetation on the Sunda Shelf, South China Sea, during the Last Glacial Maximum[J]. *Palaeogeography, Palaeoclimatology, Palaeoecology*, 2009, 278(1):88-97.
- [18] Li Z, Zhang Y L, Li Y X, et al. Palynological records of Holocene monsoon change from the Gulf of Tonkin (Beibuwan), northwestern South China Sea[J]. *Quaternary Research*, 2010, 74(1):8-14.
- [19] Dai L, Weng C Y, Lu J, et al. Pollen quantitative distribution in marine and fluvial surface sediments from the northern South China Sea: New insights into pollen transportation and deposition mechanisms[J]. *Quaternary International*, 2014, 325:136-149. doi: 10.1016/j.quaint.2013.09.031.
- [20] 赵琳. 福建戴云山中晚全新世泥炭孢粉记录的植被、气候变化与人类活动[D]. 南京: 南京大学硕士学位论文, 2014: 25-62.  
Zhao Lin. Pollen Records of Vegetation, Climate Changes and Human Activities during the Mid-Late Holocene from Peat Profiles in Daiyun Mountains, Fujian Province[D]. Nanjing: The Master's Thesis of Nanjing University, 2014:25-62.
- [21] Zhao L, Ma C M, Leipe C, et al. Holocene vegetation dynamics in response to climate change and human activities derived from pollen and charcoal records from Southeastern China[J]. *Palaeogeography, Palaeoclimatology, Palaeoecology*, 2017, 485:644-660. doi: 10.1016/j.palaeo.2017.06.035.
- [22] Ma T, Zheng Z, Man M, et al. Holocene fire and forest histories in relation to climate change and agriculture development in Southeastern China[J]. *Quaternary International*, 2018, 488:30-40. doi: 10.1016/j.quaint.2017.07.035.
- [23] 庞洋, 周斌, 徐向春, 等. 中国东部季风区全新世火历史及其影响因素[J]. *第四纪研究*, 2022, 42(2):368-382.  
Pang Yang, Zhou Bin, Xu Xiangchun, et al. Holocene fire history and its influencing factors in the monsoon region of East China[J]. *Quaternary Sciences*, 2022, 42(2):368-382.
- [24] Heinrich H. Origin and consequences of cyclic ice rafting in the Northeast Atlantic Ocean during the past 130,000 years[J]. *Quaternary Research*, 1988, 29(2):142-152.
- [25] Dansgaard W, Johnsen S J, Clausen H B, et al. Evidence for general instability of past climate from a 250 kyr ice core record[J]. *Nature*, 1993, 364(6434):218-220.
- [26] Patterson W A, Edwards K J, Maguire D J. Microscopic charcoal as a fossil indicator of fire[J]. *Quaternary Science Reviews*. 1987, 6(1):3-23.
- [27] Scott A C. Charcoal recognition, taphonomy and uses in palaeoenvironmental analysis[J]. *Palaeogeography, Palaeoclimatology, Palaeoecology*, 2010, 291(2):11-39.
- [28] Daniau A L, Goni M F S, Martinez P, et al. Orbital-scale climate forcing of grassland burning in Southern Africa[J]. *Proceedings of the National Academy of Sciences of the United States of America*, 2013, 110(13):5069-5073.
- [29] Wang X, Ding Z L, Peng P A. Changes in fire regimes on the Chinese Loess Plateau since the Last Glacial Maximum and implications for linkages to paleoclimate and past human activity[J]. *Palaeogeography, Palaeoclimatology, Palaeoecology*, 2011, 315:61-74. doi: 10.1016/j.palaeo.2011.11.008.
- [30] Zhou B, Shen C D, Sun W D, et al. Elemental carbon record of paleofire history on the Chinese Loess Plateau during the last 420ka and its response to environmental and climate changes[J]. *Palaeogeography, Palaeoclimatology, Palaeoecology*, 2007, 252(3):617-625.
- [31] Zhou B, Shen C D, Sun W D, et al. Late Pliocene-Pleistocene expansion of C<sub>4</sub> vegetation in semiarid East Asia linked to increased burning[J]. *Geology*, 2014, 42(12):1067-1070.
- [32] Han Y M, An Z S, Marlon J R, et al. Asian inland wildfires driven by glacial-interglacial climate change[J]. *Proceedings of the National*

- Academy of Sciences of the United States of America, 2020, 117(10):5184–5189.
- [33] Shi Y L, Pan B L, Wei M J, et al. Wildfire evolution and response to climate change in the Yinchuan Basin during the past 1.5 Ma based on the charcoal records of the PL02 core [J]. *Quaternary Science Reviews*, 2020, 241. doi: 10.1016/j.quascirev.2020.106393.
- [34] Parsons L A. Implications of CMIP6 Projected Drying Trends for 21st Century Amazonian drought risk [J]. *Earth's Future*, 2020, 8(10). doi:10.1029/2020EF001608.
- [35] Cheng Z, Weng C, Steinke S, et al. Anthropogenic modification of vegetated landscapes in Southern China from 6,000 years ago [J]. *Nature Geoscience*, 2018, 11(12):939–943.
- [36] Cheng Z J, Weng C Y, Steinke S, et al. Marine pollen records provide perspective on coastal wetlands through Quaternary sea-level changes [J]. *Ecological Indicators*, 2021, 133. doi: 10.1016/j.ecolind.2021.108405.
- [37] Lisiecki L E, Raymo M E. A Pliocene-Pleistocene stack of 57 globally distributed benthic  $\delta^{18}\text{O}$  records [J]. *Paleoceanography and Paleoclimatology*, 2005, 20(2). doi:10.1029/2005PA001164.
- [38] Liu J G, Steinke S, Vogt C, et al. Temporal and spatial patterns of sediment deposition in the northern South China Sea over the last 50,000 years [J]. *Palaeogeography, Palaeoclimatology, Palaeoecology*, 2017, 465:212–224. doi: 10.1016/j.palaeo.2016.10.033.
- [39] Huang E Q, Chen Y R, Schefuβ E, et al. Precession and glacial-cycle controls of monsoon precipitation isotope changes over East Asia during the Pleistocene [J]. *Earth and Planetary Science Letters*, 2018, 494:1–11. doi: 10.1016/j.epsl.2018.04.046.
- [40] 姚衍桃, Harff Jan, Meyer Michael, 等. 南海西北部末次盛冰期以来的古海岸线重建 [J]. *中国科学(D辑: 地球科学)*, 2009, 39(6):753–762.  
Yao Yantao, Harff Jan, Meyer Michael, et al. Reconstruction of paleocoastlines for the northwestern South China Sea since the Last Glacial Maximum [J]. *Scientia Sinica (Series D: Earth Sciences)*, 2009, 39(6):753–762.
- [41] 吴征镒. 中国植被 [M]. 北京: 科学出版社, 1980:823–896.  
Wu Zhengyi. *Vegetation of China* [M] Beijing: Science Press, 1980: 823–896.
- [42] 焦琳琳, 常禹, 胡远满, 等. 基于 MODIS 的中国野火时空分布格局 [J]. *生态学杂志*, 2014, 33(5):1351–1358.  
Jiao Linlin, Chang Yu, Hu Yuanman, et al. Spatial and temporal distribution patterns of wildfires in China based on MODIS data [J]. *Chinese Journal of Ecology*, 2014, 33(5):1351–1358.
- [43] Mohtadi M, Cruise participants. Report and preliminary results of RV SONNE cruise SO 221. INVERS., Hongkong-Hongkong, 17. 05. 2012–07.06.2012 [R]. Fachbereich Geowissenschaften Universitat Bremen, 2012: 1–168.
- [44] Paillard D, Labeyrie L, Yiou P. Macintosh program performs time-series Analysis [J] *Eos Transactions American Geophysical Union*, 1996, 77(39): 379.
- [45] Faegri K, Kaland P E. *Textbook of Pollen Analysis* [M]. Chichester: John Wiley & Sons, 1989:76–81.
- [46] 李小强, 周新郢, 尚雪, 等. 黄土炭屑分级统计方法及其在火演化研究中的意义 [J]. *湖泊科学*, 2006, 18(5):540–544.  
Li Xiaoqiang, Zhou Xinying, Shang Xue, et al. Different size method of charcoal analysis in loess and its significance in the study of fire variation [J]. *Journal of Lake Sciences*, 2006, 18(5):540–544.
- [47] 曹艳峰, 韩军青. 运城盆地全新世时期的野火活动与生态环境演变 [J]. *干旱区资源与环境*, 2009, 23(2):125–129.  
Cao Yanfeng, Han Junqing. Wildfire activity and ecological environment change during Holocene in the Yuncheng Basin [J]. *Journal of Arid Land Resources and Environment*, 2009, 23(2):125–129.
- [48] 占长林, 曹军骥, 韩永明, 等. 古火灾历史重建的研究进展 [J]. *地球科学进展*, 2011, 26(12):1248–125.  
Zhan Changlin, Cao Junji, Han Yongming, et al. Research progress on reconstruction of paleofire history [J]. *Progress in Earth Science*, 2011, 26(12):1248–125.
- [49] Clark J S, Hussey T C. Estimating the mass flux of charcoal from sedimentary records: Effects of particle size, morphology and orientation [J]. *The Holocene*, 1996, 6(2):129–144.
- [50] Clark J S. Particle motion and the theory of charcoal analysis: Source area, transport, deposition, and sampling [J]. *Quaternary Research*, 1988, 30(1):67–80.
- [51] Turner R, Roberts N, Jones M D. Climatic pacing of Mediterranean fire histories from lake sedimentary microcharcoal [J]. *Global and Planetary Change*, 2008, 63(4):317–324.
- [52] Huang C C, Pang J L, Chen S E, et al. Charcoal records of fire history in the Holocene loess-soil sequences over the southern Loess Plateau of China [J]. *Palaeogeography, Palaeoclimatology, Palaeoecology*, 2006, 239(1–2):28–44.
- [53] Miao Y F, Jin H L, Cui J X. Human activity accelerating the rapid desertification of the Mu Us Sandy Lands, North China [J]. *Scientific Reports*, 2016, 6(1). doi: 10.1038/srep23003.
- [54] Miao Y M, Zhang D J, Cai X M, et al. Holocene fire on the northeast Tibetan Plateau in relation to climate change and human activity [J]. *Quaternary International*, 2017, 443(B):124–131.
- [55] Miao Y F, Song Y G, Li Y, et al. Late Pleistocene fire in the Ili Basin, Central Asia, and its potential links to paleoclimate change and human activities [J]. *Palaeogeography, Palaeoclimatology, Palaeoecology*, 2020, 547. doi: 10.1016/j.palaeo.2020.109700.
- [56] Crawford A J, Belcher C M. Charcoal morphometry for paleoecological analysis: The effects of fuel type and transportation on morphological parameters [J]. *Applications in Plant Sciences*, 2014, 2(8). doi: 10.3732/apps.1400004
- [57] Umbanhowar C E, Mcgrath M J. Experimental production and analysis of microscopic charcoal from wood, leaves and grasses [J]. *The Holocene*, 1998, 8(3):341–346
- [58] 王梓莎, 赵永涛, 苗运法, 等. 以孢粉学方法为例浅论黄土沉积物中微体炭屑的统计问题 [J]. *干旱区地理*, 2020, 43(3):661–670.  
Wang Zisha, Zhao Yongtao, Miao Yunfa, et al. Statistical problem of microcharcoal in loess sediments based on the pollen methodology [J]. *Arid Land Geography*, 2020, 43(3):661–670.
- [59] Duffin K I. The representation of rainfall and fire intensity in fossil pollen and charcoal records from a South African savanna [J]. *Review of Palaeobotany and Palynology*, 2008, 151(1):59–71.
- [60] 张健平, 吕厚远. 现代植物炭屑形态的初步分析及其古环境意义 [J]. *第四纪研究*, 2006, 26(5):857–863.  
Zhang Jianping, Lü Houyuan. Preliminary study of charcoal morphology and its environmental significance [J]. *Quaternary Sciences*, 2006, 26(5):857–863.
- [61] Genet M, Daniua A L, Mouillot F, et al. Modern relationships between microscopic charcoal in marine sediments and fire regimes on adjacent landmasses to refine the interpretation of marine paleofire records: An Iberian case study [J]. *Quaternary Science Reviews*,

- 2021, 270. doi: 10.1016/j.quascirev.2021.107148.
- [62] Wang Z S, Miao Y F, Zou Y G, et al. Microcharcoals reveal more grass than trees during the Mid-Holocene Optimum on the Chinese Loess Plateau[J]. *Geophysical Research Letters*, 2023, 50(17).doi: 10.1029/2023GL103637.
- [63] Simpson G L. Modelling palaeoecological time series using generalised additive models[J]. *Frontiers in Ecology and Evolution*, 2018, 6. doi: 10.3389/fevo.2018.00149
- [64] Higuera P E, Brubaker L B, Anderson P M, et al. Vegetation mediated the impacts of postglacial climate change on fire regimes in the south central Brooks Range, Alaska[J]. *Ecological Monographs*, 2009, 79(2):201-219.
- [65] Hammer  $\phi$ vind. PAST:Paleontological statistics software package for education and data analysis [J]. *Palaeontologia Electronica*, 2001, 4(1):9.
- [66] Press W H, Teukolsky S A, Vetterling W T, et al. Numerical Recipes in C: The Art of Scientific Computing [M]. Cambridge: Cambridge University Press, 1992: 581-584.
- [67] Torrence C, Compo G P. A practical guide to wavelet analysis [J]. *Bulletin of the American Meteorological Society*, 1998, 79(1):61-78.
- [68] Power M J, Marlon J, Ortiz N, et al. Changes in fire regimes since the Last Glacial Maximum: An assessment based on a global synthesis and analysis of charcoal data[J]. *Climate Dynamics*, 2008, 30(7-8): 887-907.
- [69] 杜建峰, 王宁练, 李建勇, 等. 洛阳盆地全新世炭屑记录及其古环境意义[J]. *第四纪研究*, 2022, 42(2):383-396.  
Du Jianfeng, Wang Ninglian, Li Jianyong, et al. Charcoal records of Holocene loess-soil sequences and palaeoenvironmental significance in the Luoyang Basin[J]. *Quaternary Sciences*, 2022, 42(2):383-396.
- [70] Nichols G J, Cripps J A, Collinson M E, et al. Experiments in waterlogging and sedimentology of charcoal: Results and implications [J]. *Palaeogeography, Palaeoclimatology, Palaeoecology*, 2000, 164(1):43-56.
- [71] 俞心婷, 任健, 边叶萍, 等. 东西伯利亚陆架炭屑分布特征及其控制因素[J]. *极地研究*, 2024, 36(2):113-127.  
Yu Xinting, Ren Jian, Bian Yeping, et al. Charcoal distribution in surface sediments of the East Siberian Shelf and its controlling factors [J]. *Chinese Journal of Polar Research*, 2024, 36(2):113-127.
- [72] Luo C X, Chen M H, Xiang R, et al. Modern pollen distribution in marine sediments from the northern part of the South China Sea[J]. *Marine Micropaleontology*, 2014, 108:41-56. doi: 10.1016/j.mar-micro.2014.03.001.
- [73] Dai L, Weng C Y, Mao L M. Patterns of vegetation and climate change in the northern South China Sea during the last glaciation inferred from marine palynological records [J]. *Palaeogeography, Palaeoclimatology, Palaeoecology*, 2015, 440:249-258. doi: 10.1016/j.palaeo.2015.08.041.
- [74] Dai L, Weng C Y, Lu J, et al. Pollen quantitative distribution in marine and fluvial surface sediments from the northern South China Sea: New insights into pollen transportation and deposition mechanisms [J]. *Quaternary International*, 2014, 325:136-149. doi: 10.1016/j.quaint.2013.09.031.
- [75] Yu S H, Zheng Z, Chen F, et al. A last glacial and deglacial pollen record from the northern South China Sea: New insight into coastal-shelf paleoenvironment[J]. *Quaternary Science Reviews*, 2017, 157: 114-128. doi: 10.1016/j.quascirev.2016.12.012.
- [76] Dupont L. Orbital scale vegetation change in Africa [J]. *Quaternary Science Reviews*, 2011, 30(25-26):3589-3602.
- [77] Moss P T, Kershaw A P, Grindrod J. Pollen transport and deposition in riverine and marine environments within the humid tropics of Northeastern Australia [J]. *Review of Palaeobotany and Palynology*, 2004, 134(1):55-69.
- [78] Beaudouin C, Suc J, Escarguel G, et al. The significance of pollen signal in present-day marine terrigenous sediments: The example of the Gulf of Lions (western Mediterranean Sea) [J]. *Géobios*, 2006, 40(2):159-172.
- [79] Grant K M, Rohling E J, Bar-Matthews M, et al. Rapid coupling between ice volume and polar temperature over the past 150,000 years [J]. *Nature*, 2012, 491(7426):744-747.
- [80] 韩晓丽, 孙爱芝, 强杨, 等. 金佛山 4 种植物群落下表土炭屑特征初步分析[J]. *西南师范大学学报(自然科学版)*, 2011, 36(6):19-23.  
Han Xiaoli, Sun Aizhi, Qiang Yang, et al. A preliminary study of charcoal characteristics from the surface soil under four different vegetations in the Jinfo Mountains [J]. *Journal of Southwest China Normal University(Natural Science Edition)*, 2011, 36(6):19-23.
- [81] 李成, 李戈, 李仁成, 等. 植物燃烧微炭屑与植硅体的比值研究[J]. *微体古生物学报*, 2019, 36(1):79-86.  
Li Cheng, Li Ge, Li Rencheng, et al. Study on the ratio of microcharcoal particles to phytoliths derived from plant combustion [J]. *Acta Micropalaeontologica Sinica*, 2019, 36(1):79-86.
- [82] Chen C, Huang K, Zheng Z, et al. Savanna/rainforest dynamics and hydroclimate changes in northern boundary of tropical Asia over the past 150 kyrs [J]. *Global and Planetary Change*, 2023, 228. doi: 10.1016/j.gloplacha.2023.104204.
- [83] Zhang X, Zheng Z, Huang K Y, et al. Quantification of Asian monsoon variability from 68 ka BP through pollen-based climate reconstruction [J]. *Science Bulletin*, 2023, 68(7):713-722.
- [84] Bereiter B, Eggleston S, Schmitt J, et al. Revision of the EPICA Dome C CO<sub>2</sub> record from 800 to 600 kyr before present [J]. *Geophysical Research Letters*, 2015, 42(2):542-549.
- [85] 黄恩清. 中更新世以来东亚冬季风海陆记录对比 [J]. *第四纪研究*, 2015, 35(6):1331-1341.  
Huang Enqing. A comparison of the East Asia winter monsoon reconstructions from terrestrial and marine sedimentary records since the Mid-Pleistocene [J]. *Quaternary Sciences*, 2015, 35(6):1331-1341.
- [86] 张潇, 黄康有, 贾鑫, 等. 末次冰期以来中国西南地区火灾活动历史及其对植被生态系统的影响 [J]. *第四纪研究*, 2024, 44(1):59-71.  
Zhang Xiao, Huang Kangyou, Jia Xin, et al. Reconstructing the historical fire activity and its influence on the vegetation ecosystem in Southwest China since the last glacial period [J]. *Quaternary Sciences*, 2024, 44(1):59-71.
- [87] 罗运利, 孙湘君, 陈怀成. 南海北部地区百万年以来的天然火与气候: ODP1144 孔深海沉积中的炭屑记录 [J]. *科学通报*, 2006, 51(8):942-950.  
Luo Yunli, Sun Xiangjun, Chen Huaicheng. Millions of years of natural fire in north South China Sea areas and climate: ODP1144 [J]. *Chinese Science Bulletin*, 2006, 51(8):942-950.
- [88] Cheng T Z, Zou J J, Shi X F, et al. Climate-driven changes in high-intensity wildfire on orbital timescales in Eurasia since 320 ka [J]. *Lithosphere*, 2022, 9. doi: 10.2113/2022/7562666.
- [89] 王梓莎, 苗运法, 赵永涛, 等. 柴达木盆地北缘湖泊表层沉积物炭屑特征及其环境意义 [J]. *中国沙漠*, 2020, 40(4): 10-17.

- Wang Zisha, Miao Yunfa, Zhao Yongtao, et al. Characteristics of microcharcoal in the lake surface sediments in the northern margin of Qaidam Basin of China and its environmental significance[J]. *Journal of Desert Research*, 2020, 40(4):10-17.
- [90] 秦鼎, 沈才明, 蒙红卫, 等. 滇东北现代花粉/炭屑组合与植被和火灾关系[J]. *云南师范大学学报(自然科学版)*, 2018, 38(3):70-78.
- Qin Ding, Shen Caiming, Meng Hongwei, et al. Relationships between modern pollen/charcoal assemblages and vegetation/fire in Northeast Yunnan[J]. *Journal of Yunnan Normal University (Natural Sciences Edition)*, 2018, 38(3):70-78.
- [91] 刘赵东. 北京地区不同森林类型地表可燃物载量及影响因子研究[D]. 北京: 北京林业大学硕士学位论文, 2019:1-52.
- Liu Zhaodong. Study on Surface Fuel Loading and Influence Factors of Different Forest Types in Beijing Area[D]. Beijing: The Master's Thesis of Beijing Forestry University, 2019:1-52.
- [92] 李颖, 严思晓, 张秀芳, 等. 武夷山国家公园内 4 种森林类型地表可燃物热值特征比较[J]. *应用与环境生物学报*, 2020, 26(6):1385-1391.
- Li Ying, Yan Sixiao, Zhang Xiufang, et al. Comparison of surface fuel calorific value characteristics of four forest types in Wuyishan National Park [J]. *Chinese Journal of Applied and Environmental*, 2020, 26(6):1385-1391.
- [93] 王庆飞, 郝泽周, 李乐, 等. 广州城市森林主要林型可燃物空间分布与燃烧性等级分析 [J/OL]. *生态学杂志*, 1-14 [2024-11-26]. <http://kns.cnki.net/kcms/detail/21.1148.Q.20241111.1449.006.html>.
- Wang Qingfei, Hao Zezhou, Li Le, et al. Combustibility of forest fuel and fire risk class of main urban forest types in Guangzhou City[J]. *Chinese Journal of Ecology*, 1-14 [2024-11-26]. <http://kns.cnki.net/kcms/detail/21.1148.Q.20241111.1449.006.html>.
- [94] Laskar J, Robutel P, Joutel F, et al. A long-term numerical solution for the insolation quantities of the Earth[J]. *Astronomy & Astrophysics*, 2004, 428(1):261-285.
- [95] Guo F, Clemens S C, Wang T, et al. Monsoon variations inferred from high-resolution geochemical records of the Linxia loess/paleosol sequence, western Chinese Loess Plateau [J]. *Catena*, 2021, 198. doi: 10.1016/j.catena.2020.105019.
- [96] Cheng H, Edwards R L, Sinha A, et al. The Asian monsoon over the past 640,000 years and ice age terminations [J]. *Nature*, 2016, 534(7609):640-646.
- [97] 李建如, 汪品先. 南海 20 万年来的碳同位素记录[J]. *科学通报*, 2006, 51(12):1482-1486.
- Li Jianru, Wang Pinxian. Carbon isotope records from the South China Sea over 200,000 years[J]. *Chinese Science Bulletin*, 2006, 51(12):1482-1486.
- [98] 田军, 汪品先. 深海记录中的热带过程及其周期性[J]. *地球科学*, 2006, 31(6):747-753.
- Tian Jun, Wang Pinxian. Tropical process and its periodicity in the deep sea records[J]. *Earth Science*, 2006, 31(6):747-753.
- [99] Wehausen R, Brumsack H J. Astronomical forcing of the East Asian monsoon mirrored by the composition of Pliocene South China Sea sediments[J]. *Earth and Planetary Science Letters*, 2002, 201(3-4):621-636.
- [100] Wang Y J, Cheng H, Edwards R L, et al. Millennial- and orbital-scale changes in the East Asian monsoon over the past 224,000 years [J]. *Nature*, 2008, 451(7182):1090-1093.
- [101] Sun Y B, Clemens S C, An Z S, et al. Astronomical timescale and palaeoclimatic implication of stacked 3.6-Myr monsoon records from the Chinese Loess Plateau[J]. *Quaternary Science Reviews*, 2005, 25(1/2):33-48.
- [102] Maher B A. Palaeoclimatic records of the loess/paleosol sequences of the Chinese Loess Plateau [J]. *Quaternary Science Reviews*, 2016, 154:23-84. doi: 10.1016/j.quascirev.2016.08.004.
- [103] Ao H, Liebrand D, Dekkers J M, et al. Orbital- and millennial-scale Asian winter monsoon variability across the Pliocene-Pleistocene glacial intensification [J]. *Nature Communications*, 2024, 15(1):3364.
- [104] Hinnov L A. Astronomical metronome of geological consequence [J]. *Proceedings of the National Academy of Sciences of the United States of America*, 2018, 115(24):6104-6106.
- [105] Archibald S, Scholes R J, Roy D P, et al. Southern African fire regimes as revealed by remote sensing [J]. *International Journal of Wildland Fire*, 2010, 19(7):861-878.
- [106] Brockett B H, Biggs H C, van Wilgen B W. A patch mosaic burning system for conservation areas in Southern African savannas [J]. *International Journal of Wildland Fire*, 2001, 10(2):169-183.
- [107] van Wilgen B W, Biggs H C, O'Regan S P, et al. A fire history of the savanna ecosystems in the Kruger National Park, South Africa, between 1941 and 1996[J]. *South African Journal of Science*, 2000, 96(4):167-178.
- [108] Saha M V, Scanlon T M, D'Odorico P. Climate seasonality as an essential predictor of global fire activity [J]. *Global Ecology and Biogeography*, 2019, 28(2):198-210.
- [109] Zhang Z H, Wang C S, Lv D W, et al. Precession-scale climate forcing of peatland wildfires during the early Middle Jurassic Greenhouse Period[J]. *Global and Planetary Change*, 2020, 184. doi: 10.1016/j.gloplacha.2019.103051.
- [110] Bradley R S, Diaz H F. Late Quaternary abrupt climate change in the tropics and sub-tropics: The continental signal of tropical hydroclimatic events (THEs) [J]. *Reviews of Geophysics*, 2021, 59(4). doi: 10.1029/2020RG000732.
- [111] 刘亮, 杨艺凝, 许姗, 等. 辽南晚更新世风成沉积序列与古气候意义[J]. *第四纪研究*, 2024, 44(2):380-393.
- Liu Liang, Yang Yining, Xu Shan, et al. Late Pleistocene aeolian sequence and paleoclimatic significance in southern Liaoning, China [J]. *Quaternary Sciences*, 2024, 44(2):380-393.
- [112] 卢淑娟, 王芳, 刘宏, 等. 基于洞穴钙板碳、氧同位素和  $\Delta 47$  温标的青藏高原东南缘 MIS7.2 时段气候变化过程与机制探讨[J]. *第四纪研究*, 2022, 42(4):978-990.
- Lu Shuxian, Wang Fang, Liu Hong, et al. Climate change during Marine Isotope Stage 7.2 (MIS 7.2) recorded by carbon, oxygen and clumped isotope in cave flowstone from southeastern Tibetan Plateau [J]. *Quaternary Sciences*, 2022, 42(4):978-990.
- [113] Zhang Y, Cui Q Y, Blockley S, et al. Fire history in the Qinling Mountains of East-Central China since the Last Glacial Maximum[J]. *Geophysical Research Letters*, 2023, 50(10). doi: 10.1029/2023GL102848.
- [114] Engber Eamon A, Varner J, Morgan III. Patterns of flammability of the California oaks: The role of leaf traits [J]. *Canadian Journal of Forest Research*, 2012, 42(11):1965-1975.
- [115] Ivory J S, Russell J. Climate, herbivory, and fire controls on tropical African forest for the last 60 ka [J]. *Quaternary Science Reviews*, 2016, 148:101-114. doi: 10.1016/j.quascirev.2016.07.015.

- [116] Mann D P, Wiedenbeck J K, Dey D C, et al. Evaluating economic impacts of prescribed fire in the central Hardwood region[J]. *Journal of Forestry*, 2020, 118(3):275–288.
- [117] 雷秋景, 谭志海, 张琪, 等. 青海东部上喇家村黄土剖面全新世野火历史及人类活动[J]. *第四纪研究*, 2024, 44(1):72–83.
- Lei Qiuqing, Tan Zhihai, Zhang Qi, et al. Holocene fire history and human activities at Shanglajia archaeological site in eastern Qinghai Province of China[J]. *Quaternary Sciences*, 2024, 44(1):72–83.
- [118] 贾宝岩, 肖霞云, 迟长婷. 云南洱海炭屑记录揭示的近千年来古火演化历史[J]. *第四纪研究*, 2024, 44(1):158–173.
- Jia Baoyan, Xiao Xiayun, Chi Changting. Fire history over the past millennium revealed by the charcoal record from Lake Erhai, northwestern Yunnan Province[J]. *Quaternary Sciences*, 2024, 44(1):158–173.
- [119] Beaufort L, Garidel-Thoron D T, Linsley B, et al. Biomass burning and oceanic primary production estimates in the Sulu Sea area over the last 380 kyr and the East Asian monsoon dynamics [J]. *Marine Geology*, 2003, 201(1):53–65.
- [120] Thevenon F, Bard E, Williamson D, et al. A biomass burning record from the West Equatorial Pacific over the last 360 ky; Methodological, climatic and anthropic implications [J]. *Palaeogeography, Palaeoclimatology, Palaeoecology*, 2004, 213(1):83–99.
- [121] Kershaw P, van der K S, Moss P, et al. Environmental change and the arrival of people in the Australian region [J]. *Before Farming*, 2006, (1):1–24.
- [122] Guedes J D, Austermann J, Mitrovica J X. Lost foraging Opportunities for East Asian hunter-gatherers due to rising sea level since the Last Glacial Maximum [J]. *Geoarchaeology*, 2016, 31(4):255–266.

## MARINE SEDIMENTARY RECORDS REVEAL PALEOFIRE HISTORY AND ITS DRIVING MECHANISMS IN THE NORTHERN SOUTH CHINA SEA DURING THE LAST GLACIAL

XU Han<sup>1</sup>, CHENG Zhongjing<sup>2</sup>, LIU Yan<sup>1</sup>, WENG Chengyu<sup>2</sup>,  
Stephan STEINKE<sup>3</sup>, Mahyar MOHTADI<sup>4</sup>, SUN Qianli<sup>1</sup>

(1. State Key Laboratory of Estuarine and Coastal Research, East China Normal University, Shanghai 200241, China; 2. State Key Laboratory of Marine Geology, Tongji University, Shanghai 20009, China; 3. State Key Laboratory of Marine Environmental Science, Xiamen University, Xiamen 361005, China; 4. MARUM-Center for Marine Environmental Sciences, University of Bremen, Bremen D28359, Germany)

### Abstract

Fire plays a crucial role in the Earth system and has significant impacts on climate change, vegetation succession and carbon cycling but its influencing factors are complex and diverse, exhibiting strong spatial heterogeneity globally. In the tropical/subtropical regions of Asia, there remains considerable divergence in understanding the driving mechanisms of wildfires. This study analyses charcoal from 85 marine sediment samples from the GeoB16602 site (18°57'N, 113°42'36"E; 953 m in water depth) in the northern South China Sea to reconstruct the paleofire evolution sequence over the past 65~18 ka, with core depth ranging from 9.47 m to 2.91 m in core combining with pollen data. The results indicate that charcoal concentration generally shows an increasing trend as the climate become drier and herbaceous plants expand. Meanwhile, the charcoal concentration exhibits a distinct ca. 19 ka cyclic variation. During periods of low precession values, summer insolation in the tropical/subtropical regions of the Northern Hemisphere becomes stronger (while winter insolation weakens), leading to enhanced climate seasonality and increased wildfire occurrence. Conversely, during periods of high precession values, wildfire activity decreases. This may suggest that, compared to ecosystem changes (such as the ratio of herbaceous to woody plants), fire is more sensitive to climatic seasonality driven by solar insolation. Additionally, an anomalous peak in charcoal concentration is observed at 53 cal. ka B.P., which we hypothesize may be related to human activities during periods of low sea level. This record highlights the varying response patterns between wildfires and climate across different timescales and climate amplitudes, emphasizing the need to account for these dynamics in future wildfire prediction efforts.

**Key words:** vegetation; charcoal; paleofires; seasonality; precession